

Borehole velocity-prediction models and estimation of fluid saturation effects

Zandong Sun, Stephen R. Stretch and R. James Brown

ABSTRACT

Three types of elastic-wave velocity-prediction models were analyzed by means of well logs and seismic section ties by considering fluid saturation in five wells which include two different reservoir types, clastic and carbonate, in two different areas.

The bulk and shear moduli of a formation are functions of the bulk and shear moduli of the matrix and fluid components. By using the volumes of different minerals and fluids obtained from log analysis, bulk and shear moduli of the matrix and fluid were calculated. The nature of the matrix, the fluid, and the pore geometry are the critical factors in computing the velocities of a porous rock formation. The time-average equation, the Gassmann equation, and the Toksöz-Kuster model were all applied in order to find a best velocity-prediction model. Fluid saturation parameters for both invaded and uninvaded zones can be obtained from log analysis; and there are significant changes in velocities between invaded and uninvaded zones.

A comparison of different models has been carried out, and the Toksöz-Kuster model is found to be the best theoretical model, enabling reliable predictions of pore geometry. The Gassmann equation is found to be a good approximation; however, the time-average equation is not recommended for velocity prediction.

Comprehensive research encompassing laboratory study of core, well-log analysis, and study of seismic response is critical in setting up the criteria for identifying fluid saturation and fluid type in seismic sections.

INTRODUCTION

It is a matter of much concern whether or not the elastic-wave velocities (both P and S) can be predicted in cases where sonic logs are absent. Nuclear logs have been used to derive compressional and shear logs (Iverson and Walker, 1988). Unfortunately, the estimation from the algorithm is inaccurate; also it does not take into account fluid saturation.

Laboratory studies show that there are significant changes of elastic-wave velocity among gas-saturated, water-saturated and oil-saturated porous rocks (Figure 1) (Wang et al., 1991; Gardner et al., 1974; King, 1966; Wyllie et al., 1956; Elliott and Wiley, 1975). For the purpose of hydrocarbon exploration it is very important to see if seismic response in the reservoir formation can indicate the degree of fluid saturation and the type of saturants. Compressional and shear sonic logs are critical for tying seismic data to laboratory core measurement.

To develop velocity-prediction models that have fluid-saturation effects, we need to consider critical factors such as: rock matrix, pore geometry and fluid type and properties. The time-average equation (Wyllie et al., 1956) has been used for many years in acoustic-log interpretation as a measurement of formation porosity. It suggests that only the rock matrix and fluid properties influence the wave velocity. It does not take into account pore geometry at all. Gassmann (1951) models porous rock as made up of many frictionless spherical grains (Geertsma, 1961; Murphy et al., 1991), which may somehow represent the rock pore geometry. This is a more realistic way to approach a wave velocity for porous rocks. Also the experimental results can be better explained with the Gassmann theory than by the time-average equation (Wang et al., 1991).

The pore shapes must also play an important role in controlling the elastic moduli and seismic velocities. Pore shapes are taken into account in the model of Toksöz et al., (1976) which is hopefully the most useful model for deriving seismic velocities under reservoir conditions.

In this paper different types of velocity-prediction models are examined through well-log examples. The comparisons are made between predicted and real sonic logs. The relative effects of pore shapes and of gas/brine saturation on velocity are discussed. Pore-shape prediction has been attempted, and this has then been tested using data from petrographic imaging analysis. Velocities in the far wellbore (uninvaded zone) have also been predicted. Comparison has been carried out with synthetic seismograms from different velocity models. In addition, the possibility of determining saturating fluid (gas, oil, brine) from seismic data is also discussed.

THEORY

The compressional (V_p) and the shear (V_s) velocities of the effective medium (rock formation) are defined in terms of the effective moduli:

$$V_p = \left(\frac{K_{fm} + \frac{4}{3}\mu}{\rho} \right)^{1/2} \quad (1)$$

$$V_s = \left(\frac{\mu}{\rho} \right)^{1/2} \quad (2)$$

where K_{fm} and μ are, respectively, bulk and shear moduli of the rock formation, and ρ is density of the rock formation.

It is assumed that the media are isotropic and elastic-porous; also that the relative motion between rock grains and fluid can take place freely, which means that when rock is under a shear stress the fluid effects on the shear modulus of the formation can be neglected. A reservoir formation consists of two fractions: solid elastic matrix and saturating fluid (gas, oil, brine) in randomly distributed pores. The bulk and shear moduli of formation are functions of bulk and shear moduli of the matrix and fluid components. Theoretical formulations for elastic moduli for the solid and fluid fractions are given (Krief et al., 1990) as:

$$\frac{v_{sld}}{K_s} = \sum_{i=1}^n \frac{v_{mini}}{K_{mini}} \quad (3)$$

$$\frac{v_{sld}}{\mu_s} = \sum_{i=1}^n \frac{v_{mini}}{\mu_{mini}} \quad (4)$$

$$\frac{v_{fld}}{K_f} = \frac{v_{wf} + v_{wb}}{K_w} + \frac{v_{gas}}{K_{gas}} + \frac{v_{oil}}{K_{oil}} \quad (5)$$

where K_s and μ_s are bulk and shear moduli of the solid fraction in the formation; v_{sld} and v_{fld} are the total volumes of solid and fluid; K_{mini} , μ_{mini} and v_{mini} are bulk and shear moduli and volume of mineral i ; K_f , K_w , K_{gas} and K_{oil} are bulk moduli of fluid, water, gas and oil; v_{wf} , v_{wb} , v_{gas} and v_{oil} are the volumes of free water, bound water, gas and oil.

Time-average equation

The time-average equation (Wyllie et al., 1956) is given by the formula:

$$\frac{1}{V_{fm}} = \frac{1 - \phi}{V_{sld}} + \frac{\phi}{V_{fld}} \quad (6)$$

where ϕ is total porosity of formation. This relation does not take into account the effect of pore shape on the formation velocity. It also suggests that rock with randomly distributed pores (a composite medium) consists of a layered system of parallel alternating slices of a solid and a liquid, crossed by the wave raypath perpendicular to the interfaces (Figure 2a).

Gassmann equation

Gassmann's (1951) model suggests that rock with randomly distributed pores consists of various liquid-saturated packings of frictionless spherical grains (Figure 2b). This model is still highly idealized but it is suitable for low frequency. The theory predicts velocity in the seismic frequency range (sonic-log frequencies may be borderline). The theory of Gassmann expresses the bulk moduli of the formation and of its skeleton as functions of the bulk moduli of components of the formation (matrix, fluid) and porosity.

The compressional (V_p) velocity of the formation (composite medium) is defined in terms of bulk moduli of dry rock, solid and fluid fractions, and total porosity of the formation:

$$V_p^2 = \frac{1}{\rho} \left[\frac{(K_s - K_d)^2}{K_s \left(1 - \phi - \frac{K_d}{K_s} + \phi \frac{K_s}{K_f} \right)} + K_d + \frac{4}{3} \mu \right] \quad (7)$$

where K_d is bulk modulus of dry rock which is an unknown parameter. Applying the Biot coefficient, β , the bulk modulus of the formation can be written as:

$$K_{fm} = K_s (1 - \beta) + \beta^2 M \quad (8)$$

where the modulus M is dependent on β according to:

$$M = \frac{1}{\frac{\beta - \phi}{K_s} + \frac{\phi}{K_f}} \quad (9)$$

and, empirically, β is a function of total porosity, ϕ :

$$(1 - \beta) = (1 - \phi)^{\frac{3}{1 - \phi}} \quad (10)$$

Under the assumption of equation (8), Gassmann's equation can be simplified as the interpretation-model equation (Appendix A):

$$V_P^2 = \frac{1}{\rho} \left[(1 - \beta)(K_s + \frac{4}{3} \mu) + \beta^2 M \right] \quad (11)$$

Toksöz-Kuster Equations

It is a fact that the pore shapes play an important role in controlling the elastic moduli and seismic velocity. Laboratory study shows that for a given concentration the pores with smaller aspect ratios affect both compressional- and shear-wave velocities much more than spherical pores. Less than 1% of pores with aspect ratios of 0.01 or smaller decrease the velocity as much as 20% (Toksöz et al., 1976; Kuster and Toksöz, 1974a, b).

Unlike the time-average and the Gassmann equations, the Toksöz-Kuster model includes information on pore geometry. Based on scattering theory, Toksöz et al. (1976) developed three sets of equations for an isotropic medium with random distribution of pores: (1) single pore aspect ratio and saturated with a fluid; (2) different pore aspect ratios and saturated with a fluid, and (3) different pore aspect ratios and saturated with multiphase fluid. According to the applicability of equations, available parameters and reservoir petrophysical analysis, we used the second set of equations to predict velocity, namely:

$$\frac{K_s - K_{fm}}{3K_{fm} + 4m} = \frac{K_s - K_f}{9K_s + 12m} \sum_{m=1}^M C(a_m) T_{ijj}(a_m) \quad (12)$$

$$\frac{\mu - \mu_{fm}}{6\mu_{fm}(K_s + 2\mu_s) + \mu_s(9K_s + 8\mu_s)} = \frac{m_s}{25m_s(3K + 4m_s)} \sum_{m=1}^M C(a_m) \left[T_{ijj}(a_m) - \frac{1}{3} T_{\bar{i}\bar{j}\bar{j}}(a_m) \right] \quad (13)$$

where α is aspect ratio, $C(\alpha)$ is concentration at α , and T_{ijj} and T_{ijj} are scalar functions of K_s , μ , K_t , and α , as given by Toksöz et al. (1976). Also,

$$\phi = \sum_{m=1}^M C(\alpha_m). \quad (14)$$

CASE STUDIES

Including both clastic and carbonate reservoirs, five wells were selected from two different areas (AT and AJ) in these case studies. Three sandstone reservoir wells (A, B, C) are in area AT. Two carbonate reservoir wells (D, E) are in area AJ.

Bulk and shear moduli data of minerals were calculated from velocity and density measurement (see Appendix C). The percent volumes of different minerals and different fluids are available from log analysis based on different logs (not necessarily sonic logs) and petrographic imaging. The bulk and shear moduli of solid fraction were calculated by applying equations (3) to (5). The sonic-log tool can only measure elastic properties near the wellbore in the borehole. The fluid saturation in the near wellbore (invaded zone) is different from the far wellbore (uninvaded zone). Usually pores in the invaded zone of the reservoir are filled with water from drilling mud. Invaded-zone fluid parameters were applied to predict velocities to be compared with measured sonic logs. Predicted and measured sonic logs (both P and S) are plotted in the right-hand column in Figure 3. It is evident that both the time-average and Gassmann equations predict rather good velocities compared with measured sonic logs in this case. An anomaly occurred for the time-average equation in the high-porosity interval. The reason for this is that the time-average equation does not work well in fluid-saturated intervals.

Pore-shape effects on velocity

In order to demonstrate the effects of pore shapes on seismic velocities of porous rock, we carried out two sets of modelling with two different types of pore aspect-ratio distributions. The first model assumes that the porous rock only contain pores with one shape. Well C was selected as an example. Given the invaded-zone fluid saturation (mostly free water and bound gas and water), the P-wave slowness was calculated. Changing the pore shape from near spherical to oblate (i.e. pore aspect ratio from 0.9 to 0.1, Figure 4a), we calculated P-wave slowness. The P-wave slowness spectra are shown in Figure 4b. This indicates that: (1) decreasing pore aspect ratio increases slowness and decreases velocity; (2) under the same fluid-saturation situation, the velocity of porous rock with oblate pores is much lower than that with spherical pores, and (3) when pore aspect ratio is lower than 0.4 the velocity of the medium starts changing dramatically.

The second model was applied to the same well on the same reservoir interval as the first model. This model assumes that the porous rock contains different pore shapes (i.e. a pore aspect ratio-spectrum) with a certain concentration (Figure 5a). Changing the pore aspect ratio spectrum (dominantly from quasi-spherical to oblate pores), we calculated the P-wave slowness plotted on Figure 5b. The results indicate that the dominant pore aspect ratio in the spectrum is the main controlling factor for the rock velocity.

Pore-shape prediction, fluid-saturation effects and synthetic seismograms

The effective pore aspect ratio for both well B and well C is around 0.12, as obtained from the Toksöz-Kuster model analysis in invaded zones of the reservoir intervals. Figure 6 shows the pore aspect ratio spectrum of a typical thin section in well B from laboratory study. The dominant pore aspect ratio is around 0.166. This represents a good agreement between theoretical prediction and laboratory study.

As discussed above, the fluid saturation in the invaded zone is different from that in uninvaded zone. Well B is a typical well with a clastic reservoir (gas saturant). In the uninvaded zone, fluids are predominantly gas and, to a lesser extent, bound water/brine. The fluids in the invaded zone are mostly water/brine (from the drilling mud) with less bound gas. By using the time-average, Gassmann, and Toksöz-Kuster models, the predicted P-wave slowness in the invaded and uninvaded zones are shown in Figures 7 and 8, respectively. They indicate: (1) the time-average equation does not work well, especially in a high-porosity reservoir interval; (2) the velocity in the uninvaded zone is significantly lower than in the invaded zone.

The synthetic seismograms obtained by applying velocities predicted from different models in the uninvaded zone, are different. The form of the regional seismic (P-wave) event is shown on the right side (in the real seismic section) in Figure 9. The seismic event almost splits into two parts in the gas trap (around well B). It is low-amplitude in the upper part and high-amplitude in the lower part. The synthetic seismogram from the measured sonic log shows the reverse result in P formation (higher amplitude on upper part and lower amplitude on lower part). It is totally split into two events based on velocities predicted by the time-average equation, and it best fits the velocities predicted by the Toksöz-Kuster model.

Error analysis in velocity prediction

It is hard to determine the bulk and shear moduli of clay minerals. They are rarely documented in the literature because it is not easy to obtain pure clay minerals in nature; also there are some limitations to measuring the moduli or velocities of clay minerals. Kaolinite and illite are the components of shale; and shale is usually anisotropic in the natural condition. The bulk and shear moduli of shale change with direction of applied stress.

The second error source of velocity prediction is reservoir anisotropy. In some reservoirs, especially carbonate reservoirs, cracks or fractures sometimes are orientated in a certain direction, and velocities in different directions are different. But the sonic tool only measures acoustic properties in the direction along the borehole.

Fluids affect the shear modulus of a rock formation and, especially when fluids are bound, they strongly control the shear modulus of a formation. Therefore, they change the P- and S-wave velocities too.

According to Geertsma (1961), the acoustic wave velocity in liquid-saturated porous sediments is somewhat frequency-dependent. The effect of frequency results is less than 5% between sonic and ultrasonic-wave velocity. This factor should be taken into account when the Toksöz-Kuster model is applied.

CONCLUSIONS

The investigation of different prediction models for velocity of elastic waves in liquid-saturated porous rocks leads to the following conclusions.

Comprehensive laboratory study of core, well-log analysis, and investigation of seismic response are all critical to the establishment of criteria for identifying fluid saturation and fluid type on seismic section.

The time-average equation is based on an inadequate physical picture, especially for high-porosity intervals. The Gassmann equation is a good approximation in most cases, but does not honour the real physical nature of porous rock and, as it transpires, is not very sensitive to fluid saturation. The Toksöz-Kuster model is the best of these three models.

There are significant velocity changes for different fluid saturation, and this generates significant effects on seismograms. The Toksöz-Kuster model also provides us a way to predict pore geometry (the effective pore aspect ratio) in porous rock. There is a good agreement between the predicted pore aspect ratio (0.12) and pore aspect ratio spectrum from the laboratory study in the work area.

ACKNOWLEDGEMENTS

We would like to thank Canadian Hunter Exploration Ltd for permission to present this paper at the 1991 CREWES meeting. Tai P. Ng is thanked for providing the original suggestion and the stimulus for this research.

REFERENCES

- Bradley, H.B., et al., 1987, Petroleum Engineering Handbook: Soc. Petr. Eng.
- Gardner, G.H.F., Gardner, L.W., and Gregory, A.R., 1974, Formation velocity and density - The diagnostic basics for stratigraphic traps: *Geophysics*, **39**, 770-780.
- Carmichael, R.S., 1982, CRC Handbook of Physical Properties of Rocks: CRC Press, Inc.
- Elliott, S.E., and Wiley, B.F., 1975, Compressional velocities of partially saturated, unconsolidated sands: *Geophysics*, **40**, 949-954.
- Gassmann, F., 1951, Elastic waves through a packing of spheres: *Geophysics*, **16**, 673-685.
- Geertsma, J., 1961, Velocity-log interpretation: The effect of rock bulk compressibility: *J. Soc. Petr. Eng.*, **1**, 235-248.
- Iverson, W.P., and Walker, J.N., 1990, Shear and compressional logs derived from nuclear logs: Soc. Expl. Geophys., 58th Ann. Intl. Mtg., Expanded Abstracts, 111-113.
- King, M.S., 1966, Wave velocities in rocks as a function of changes in overburden pressure and pore fluid saturants: *Geophysics*, **31**, 50-73.
- Krief, M., Garat, J., Stellingwerff, J., and Ventre, J., 1990, A petrophysical interpretation using the velocities of P and S waves (full-waveform sonic): *The Log Analyst*, **31**, 355-369.
- Kuster, G.T., and Toksöz, M.N., 1974a, Velocity and attenuation of seismic waves in two-phase media: Part I. Theoretical formulations: *Geophysics* **39**, 588-606
- 1974b, Velocity and attenuation of seismic waves in two-phase media: Part II. Experimental results: *Geophysics* **39**, 607-618
- Murphy, W.F., Schwartz, L.M., and Hornby, B., 1991, Interpretation physics of V_P and V_S in sedimentary rocks: Soc. Prof. Well Log Anal., 32nd Ann. Logging Symp.
- Schlumberger, 1989, Log Interpretation Charts: Schlumberger Educational Services.

- Toksöz, M.N., Cheng, C.H., and Timur, A., 1976, Velocities of seismic waves in porous rocks: *Geophysics*, **41**, 621-645.
- Wang, Z., Hirsche, W.K., and Sedgwick, G., 1991, Seismic velocities in carbonate rocks: *J. Can. Petr. Tech.*, **30**, No. 2, 112-122.
- Western Atlas International, 1985, Atlas Wireline Services Log Interpretation Charts: Western Atlas Int.
- Wyllie, M.R.J., Gregory, A.R., and Gardner, L.W., 1956, Elastic wave velocities in heterogeneous and porous media: *Geophysics* **21**, 41-70.

APPENDIX A

DERIVATION OF THE INTERPRETATION-MODEL EQUATION

The basic formulations may be written as:

$$\rho V_P^2 = K_{fm} + \frac{4}{3} \mu \quad (\text{A-1})$$

and

$$\rho V_S^2 = \mu. \quad (\text{A-2})$$

We have also:

$$K_{fm} = K_s (1 - \beta) + \beta^2 M \quad (\text{A-3})$$

where

$$M = \frac{1}{\frac{\beta - \phi}{K_s} + \frac{\phi}{K_f}}. \quad (\text{A-4})$$

Substituting (A-3) into (A-1) yields:

$$\rho V_P^2 = \rho_s (V_{P_s}^2 - \frac{4}{3} V_{S_s}^2) (1 - \beta) + \beta^2 M + \frac{4}{3} \mu (1 - \beta) \quad (\text{A-5})$$

$$= \rho_s V_{P_s}^2 (1 - \beta) + \beta^2 M. \quad (\text{A-6})$$

But

$$V_{P_s}^2 = \frac{K_s + \frac{4}{3} \mu}{\rho_s} \quad (\text{A-7})$$

where V_{P_s} is P-wave velocity of the solid formation fraction. So finally:

$$V_P^2 = \frac{1}{\rho} \left[(1 - \beta) \left(K_s + \frac{4}{3} \mu \right) + \beta^2 \frac{1}{\frac{\beta - \phi}{K_s} + \frac{\phi}{K_f}} \right]. \quad (\text{A-8})$$

APPENDIX B
FROM THE GASSMAN EQUATION TO THE SIMPLIFIED MODEL
EQUATION

The Gassman equation (7) is:

$$V_p^2 = \frac{1}{\rho} \left[\frac{(K_s - K_d)^2}{K_s \left(1 - \phi - \frac{K_d}{K_s} + \phi \frac{K_s}{K_f} \right)} + K_d + \frac{4}{3} \mu \right] \quad (\text{B-1})$$

$$K_{fm} = K_s (1 - \beta) + \beta^2 \frac{1}{\frac{\beta - \phi}{K_s} + \frac{\phi}{K_f}}. \quad (\text{B-2})$$

For dry rock, $K_f \approx 0$ and $\frac{\phi}{K_f} \rightarrow \infty$, so that

$$K_d = K_s (1 - \beta). \quad (\text{B-3})$$

Thus

$$V_p^2 = \frac{1}{\rho} \left[\frac{(K_s \beta)^2}{K_s \left(\beta - \phi + \frac{\phi K_s}{K_f} \right)} + (1 - \beta) \left(K_s + \frac{4}{3} \mu \right) \right] \quad (\text{B-4})$$

$$= \frac{1}{\rho} \left[(1 - \beta) \left(K_s + \frac{4}{3} \mu \right) + \beta^2 \frac{1}{\frac{\beta - \phi}{K_s} + \frac{\phi}{K_f}} \right]. \quad (\text{B-5})$$

APPENDIX C

BULK AND SHEAR MODULI OF DIFFERENT MINERALS

Bulk and shear moduli of different minerals and fluids

Minerals	Bulk modulus ($\times 10^{10}$ kg/ms ²)	Shear modulus ($\times 10^{10}$ kg/ms ²)	Reference
Calcite	7.33000	2.66100	Carmichael (1982)
Dolomite	4.41438	3.04587	Carmichael (1982)
Quartz	3.59805	3.16715	Schlumberger (1989)
Siderite	1.14963	0.47398	Western Atlas (1985)
Brine	0.24550	————	Bradley (1987)
Natural gas	0.00396	————	Bradley (1987)
Kaolinite	3.66090*	0.94539*	unpublished
Illite	3.66090*	0.94539*	unpublished

* Kaolinite and illite are the components of shale. And shale is anisotropic in natural condition.

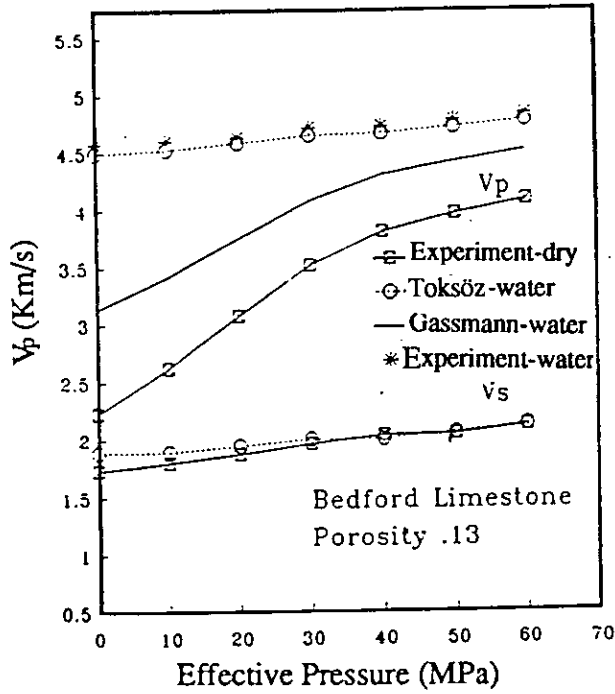


FIG. 1 Comparison of the calculated and measured velocities in Bedford limestone, computed P-wave velocity using Gassmann equation and Toksoz model, using pore aspect ratios and distributions given by Toksöz et al. (1976) (modified from Wang et al., 1991).

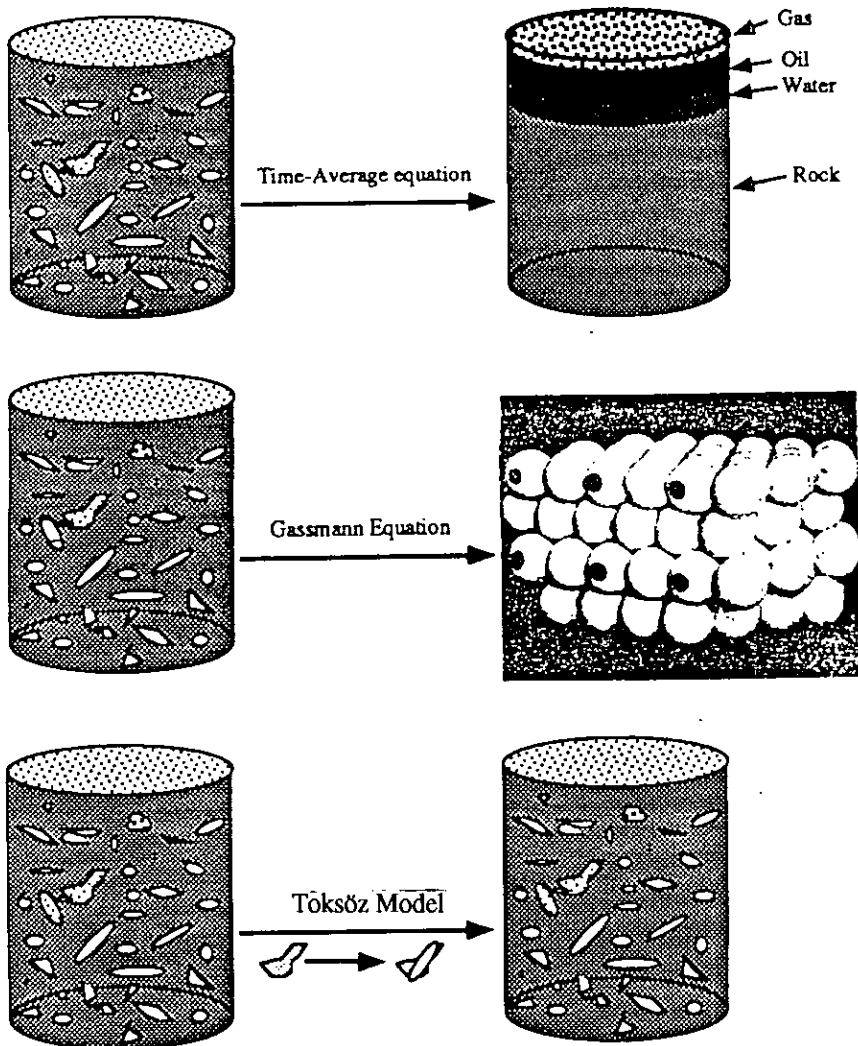


FIG. 2 Schematic diagrams showing different velocity prediction models.

- a) time-average equation: taking porous rock as layered system;
- b) Gassmann equation: taking porous rock as packings of frictionless spherical grains;
- c) Toksöz-Kuster model: including pore shape information.

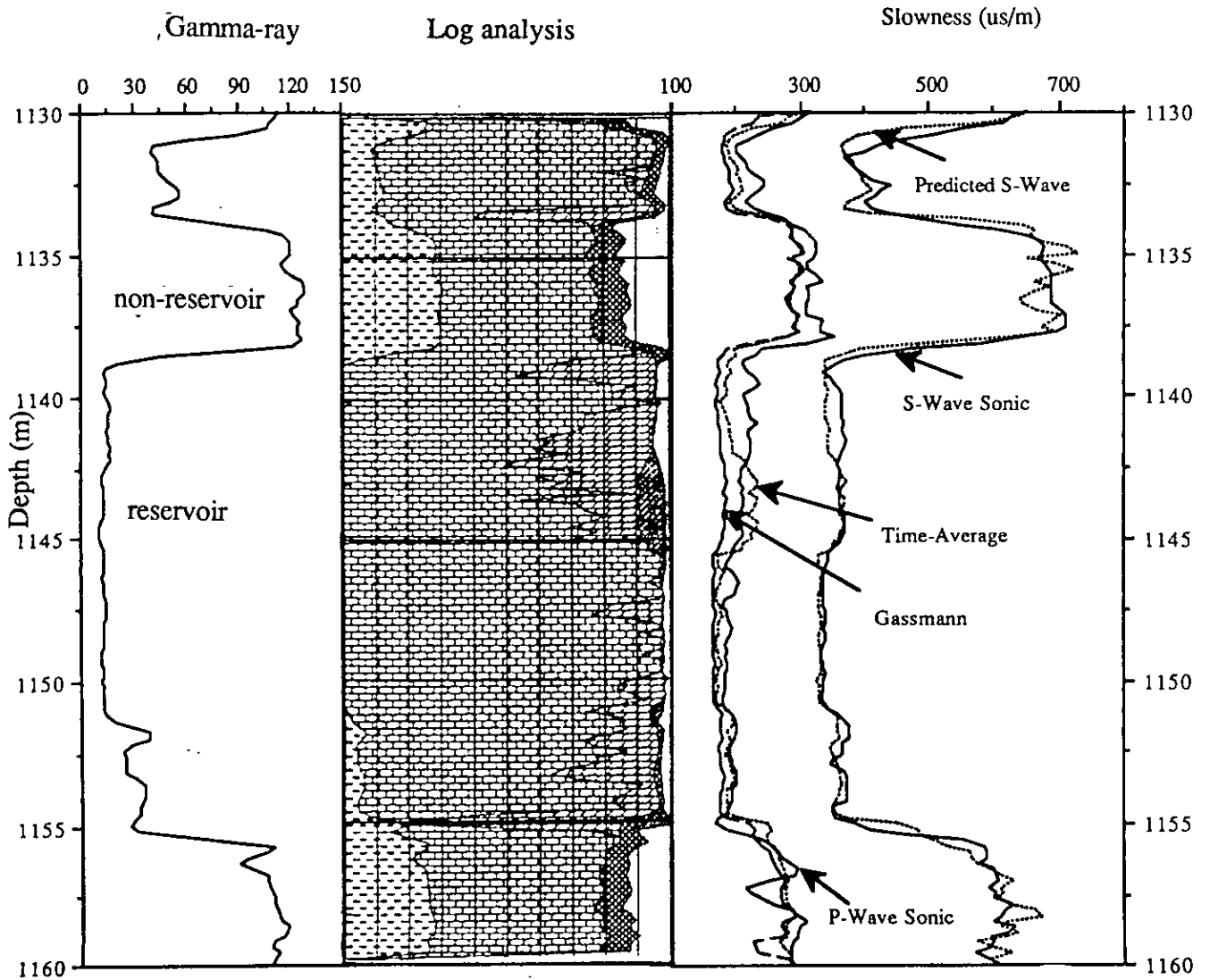
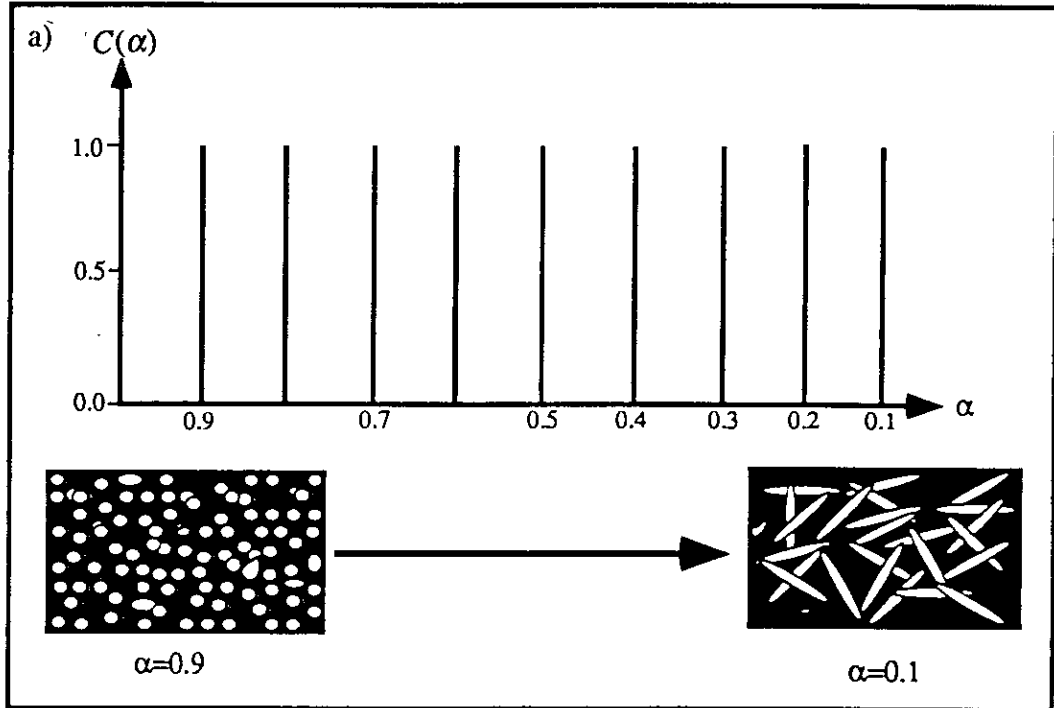
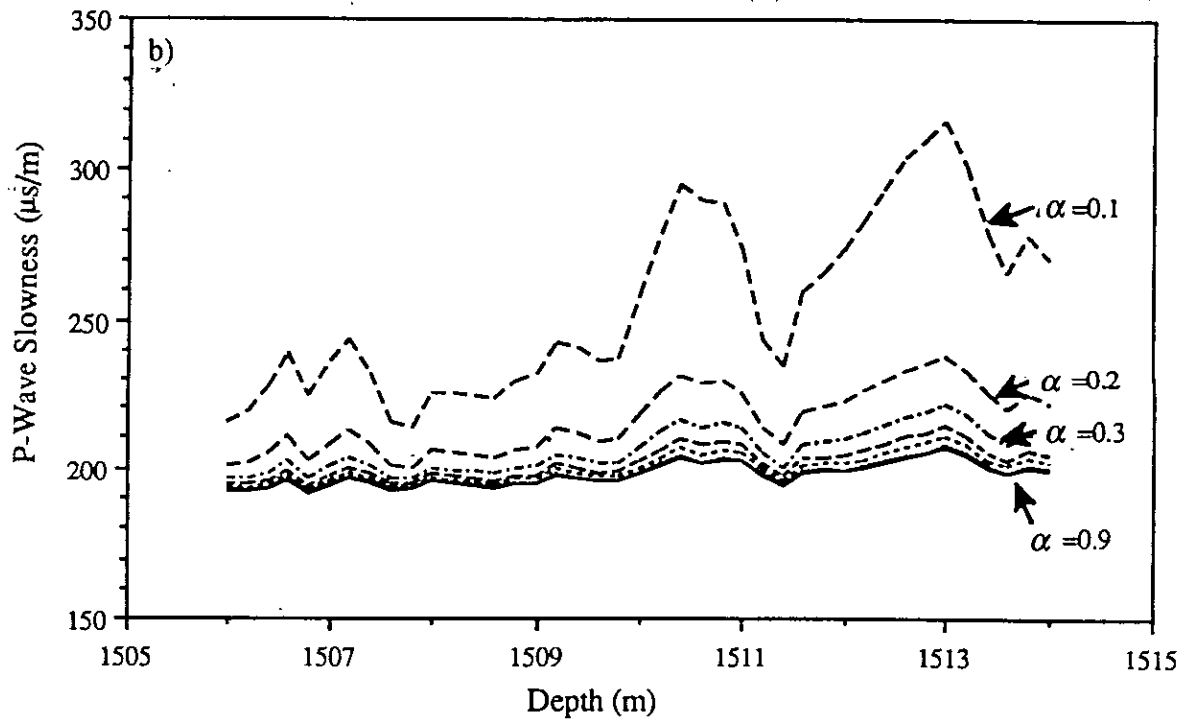


FIG. 3 Plots of predicted and measured sonic log (in right column) using time-average and Gassmann equation, log analysis result showing volumes of different minerals and fluid (middle column), and gamma log showing reservoir and non-reservoir interval (left column).

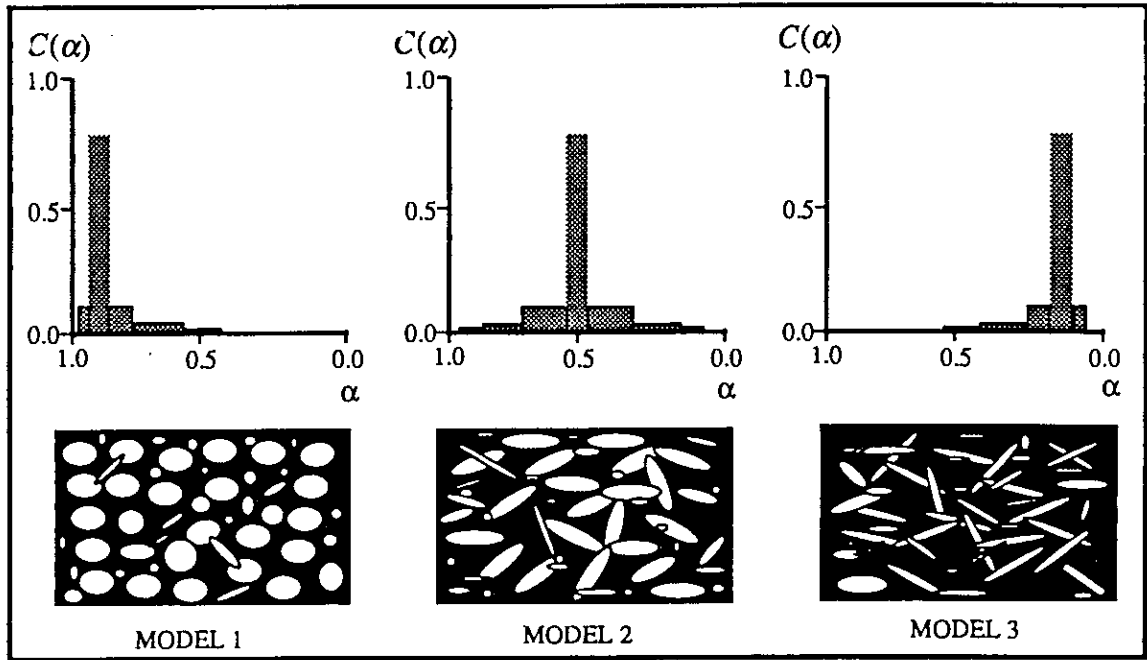


a) pore aspect-ratio spectra (single pore shape), $C(\alpha)$ is normalized concentration;

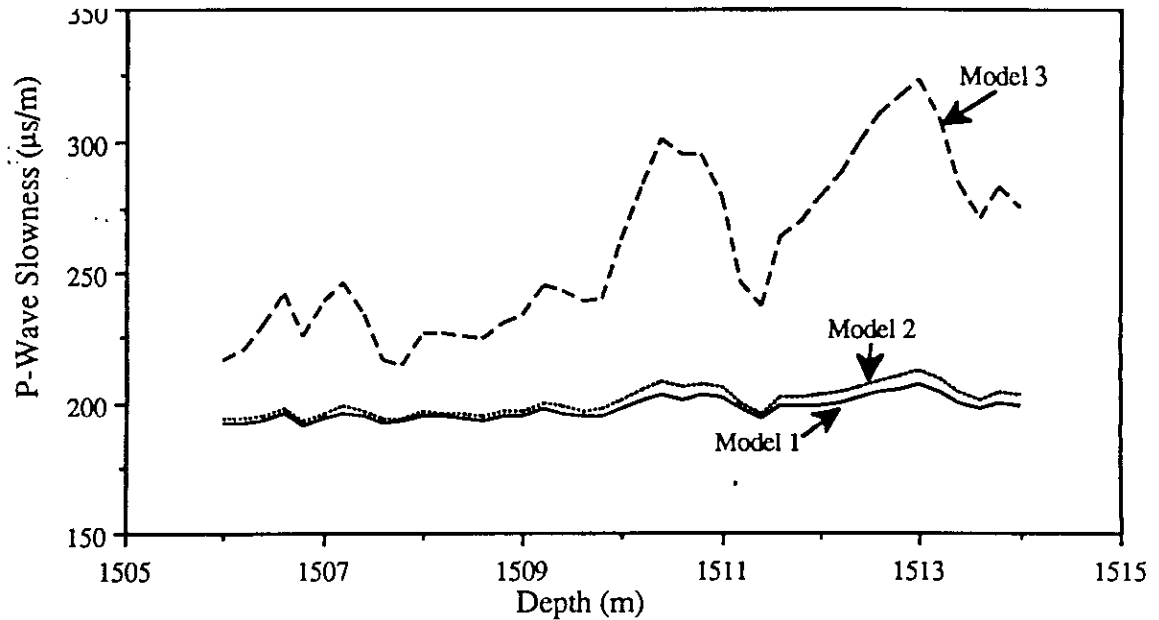


b) predicted ΔT in the wet case for different pore aspect ratios shown in (a).

FIG. 4 Plots of predicted P-wave slowness versus different pore aspect ratio (single pore shape), showing relationship between seismic velocity and pore shapes.



a) pore aspect-ratio spectra, $C(\alpha)$ is normalized concentration;



b) Predicted delta T for the models shown in (a)

FIG. 5 Plots of predicted P-wave slowness versus three pore aspect-ratio spectra, showing the relationship between seismic velocity and pore-shape distribution.

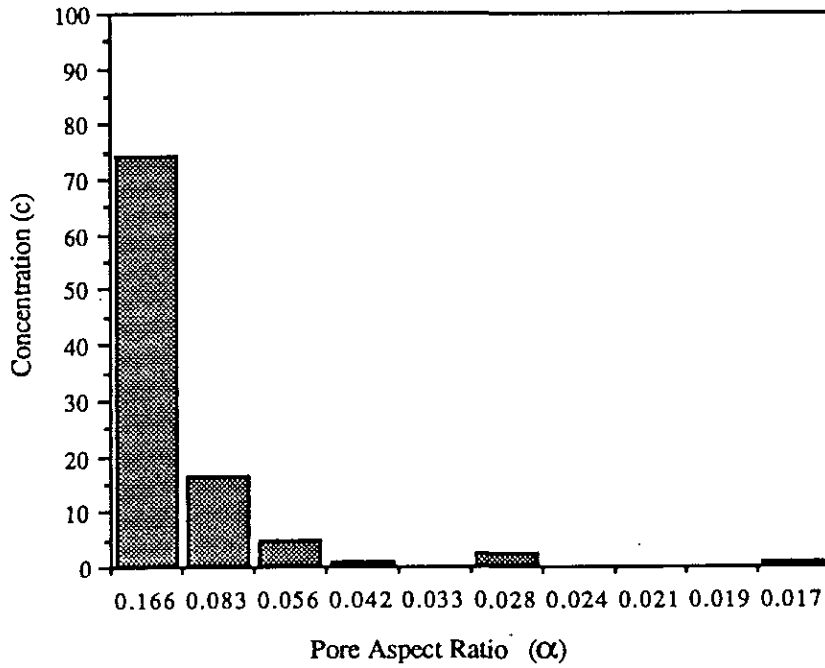


Fig. 6 Histogram of pore aspect ratio versus concentration from Petrograph Image in well B, showing the agreement of pore shape between prediction and the real.

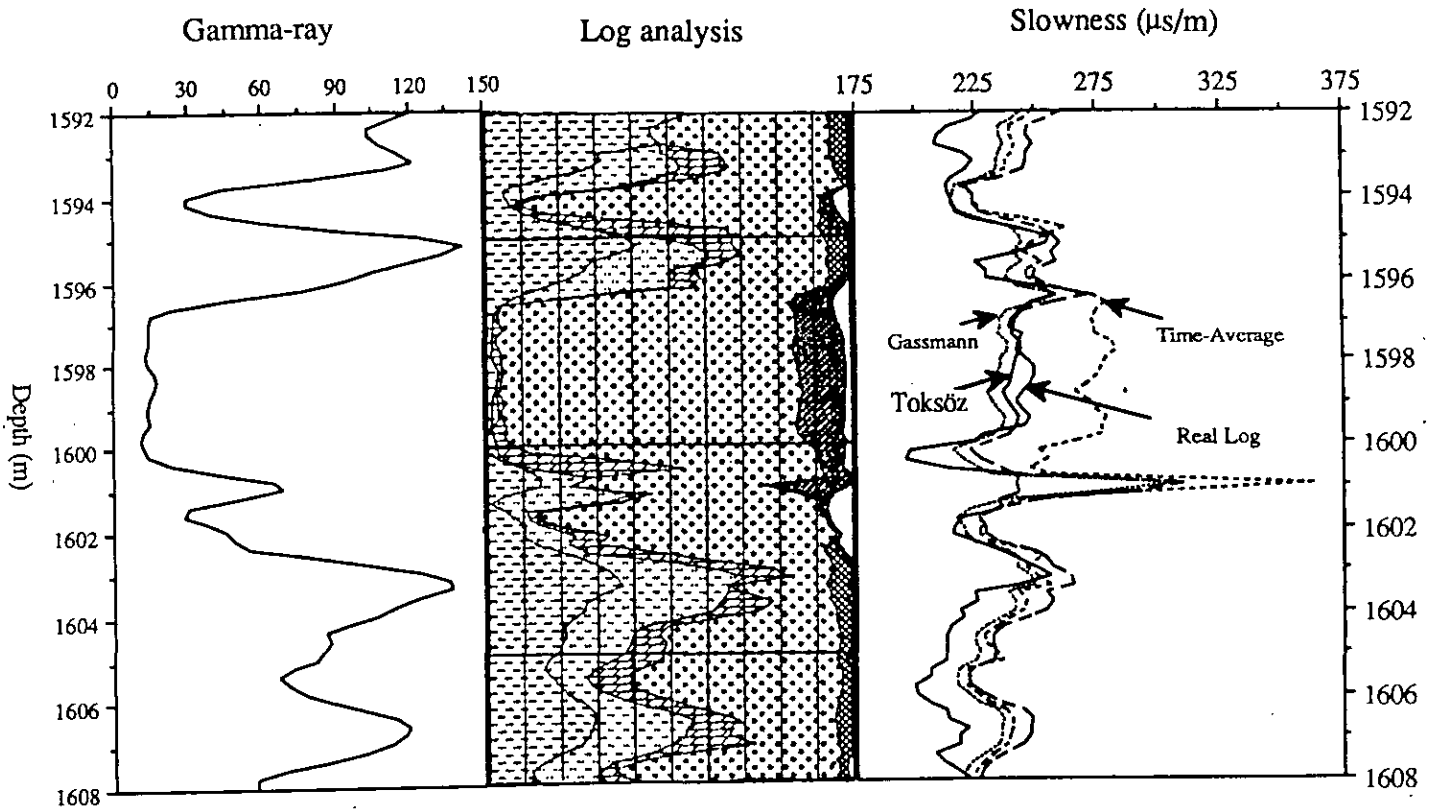


FIG. 7 Plots of predicted and measured P-wave sonic log in classical reservoir interval (right column), using time-average, Gassmann, and Toksöz-Kuster model (predicted pore aspect ratio 0.12).

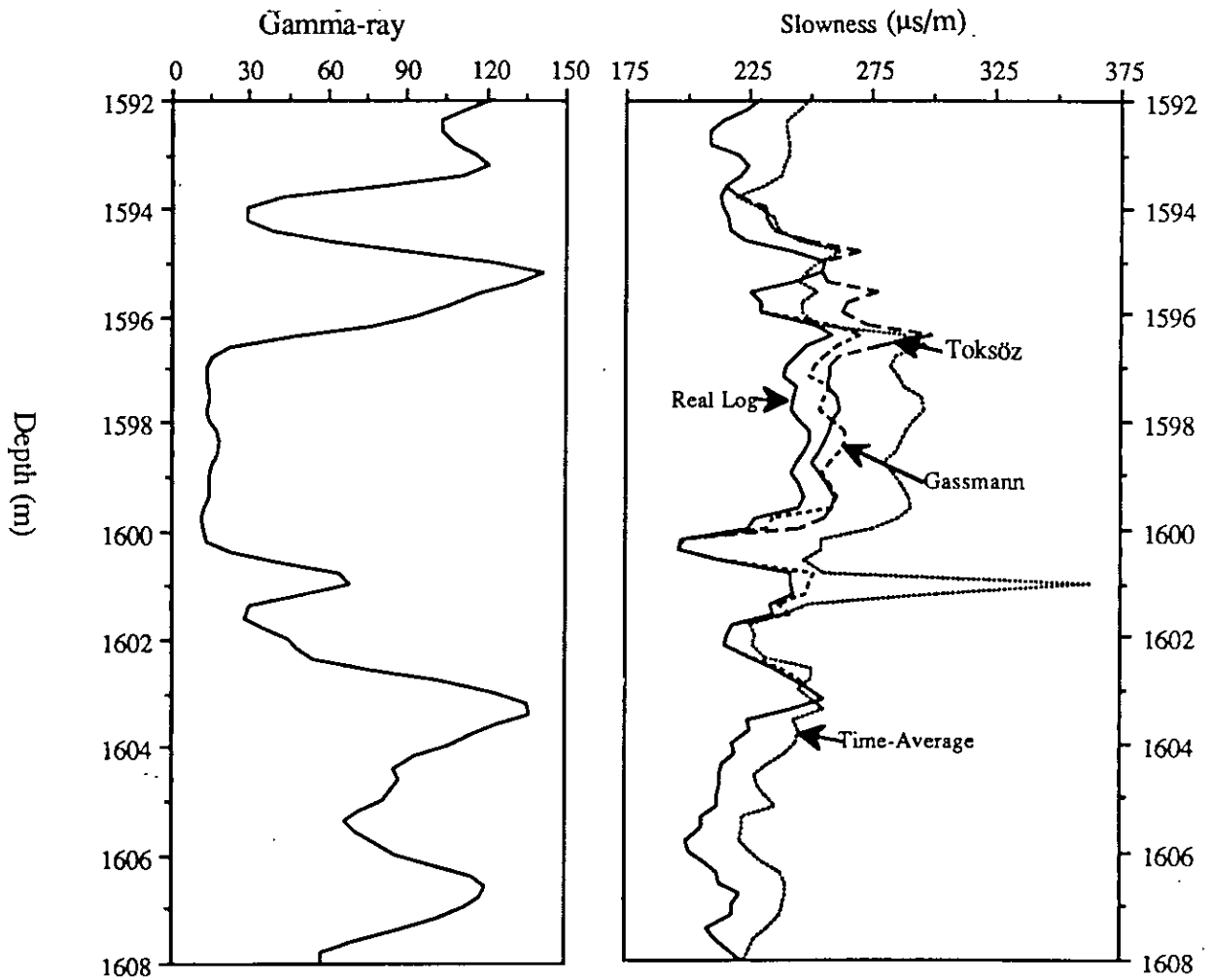
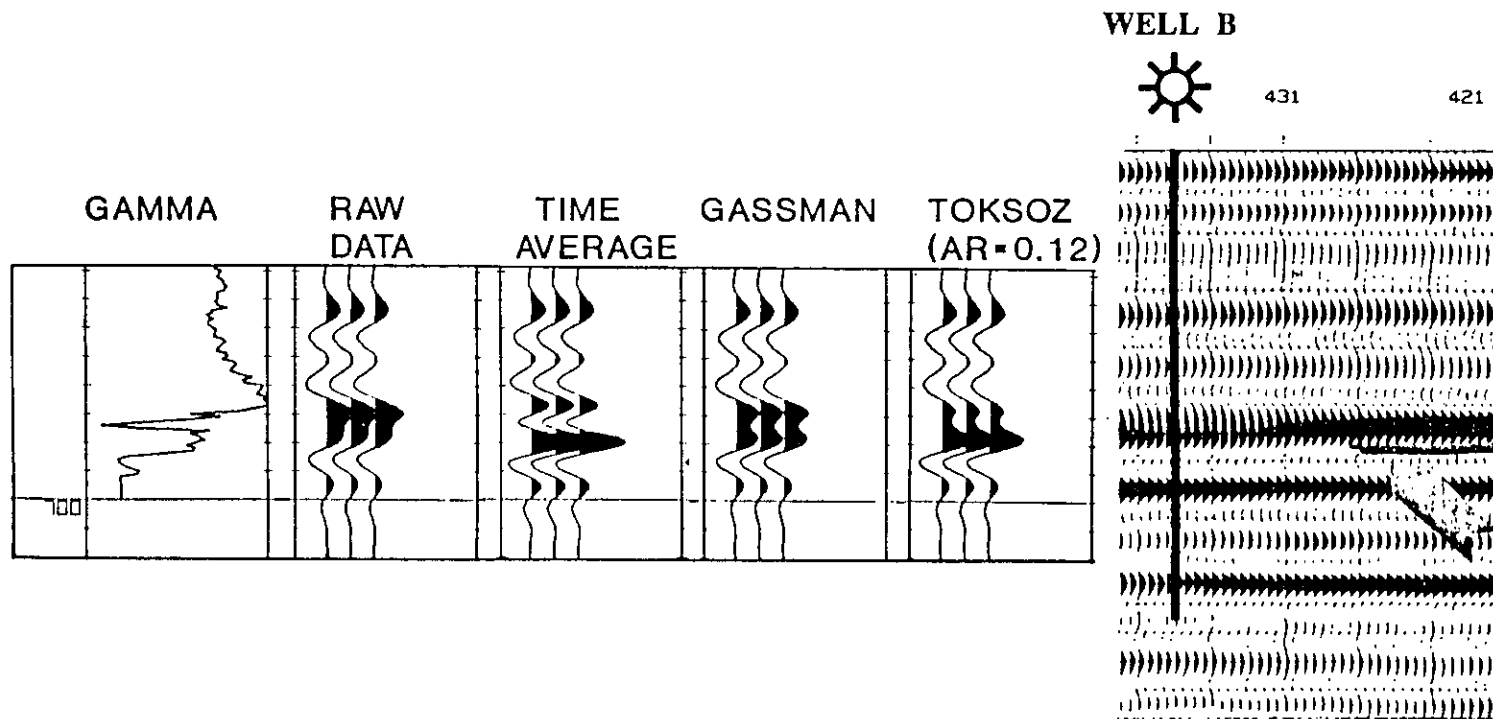


FIG. 8 Plots of predicted P-wave sonic logs in uninvasion zone in well B, using time-average, Gassmann, Toksöz-Kuster model (effective pore aspect ratio 0.12).



NOTE: 10/70 Hz BUTTERWORTH FILTER

FIG. 9 Comparison of different synthetic seismograms with real seismic section; logs used for sythetic seismograms: measured (real) log, log predicted from time-average equation, log predicted from Gassmann equation, and log predicted from Toksöz-Kuster model (all in uninvaded zone).